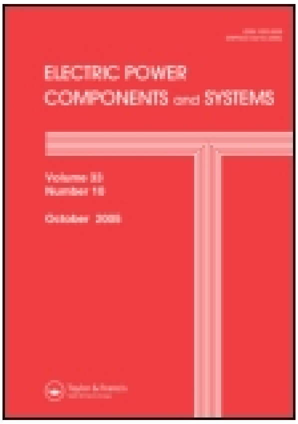

Electric Power Components and Systems
Publication details, including instructions for authors and subscription information:
http://www.tandfonline.com/loi/uemp20

Techno-economic Evaluation of Reduction of Low-voltage Bushings Diameter in Single-phase Distribution Transformers

Juan C. Olivares-Galvan [a], Salvador Magdaleno-Adame [b], Eduardo Campero-Littlewood [a], Rafael Escarela-Perez [a] & Pavlos S. Georgilakis [c]

[a] Departamento de Energia, Universidad Autonoma Metropolitana-Azcapotzalco, Mexico City, Mexico

[b] Instituto Tecnologico de Morelia, Morelia, Michoacan, Mexico

[c] School of Electrical and Computer Engineering, National Technical University of Athens (NTUA), Athens, Greece

Available online: 31 Aug 2011

Electric Power Components and Systems, 39:1388–1402, 2011

ISSN: 1532-5008 print/1532-5016 online
DOI: 10.1080/15325008.2011.584109

Techno-economic Evaluation of Reduction of Low-voltage Bushings Diameter in Single-phase Distribution Transformers

JUAN C. OLIVARES-GALVAN,[1]
SALVADOR MAGDALENO-ADAME,[2]
EDUARDO CAMPERO-LITTLEWOOD,[1]
RAFAEL ESCARELA-PEREZ,[1] and
PAVLOS S. GEORGILAKIS[3]

[1]Departamento de Energia, Universidad Autonoma Metropolitana-Azcapotzalco, Mexico City, Mexico
[2]Instituto Tecnologico de Morelia, Morelia, Michoacan, Mexico
[3]School of Electrical and Computer Engineering, National Technical University of Athens (NTUA), Athens, Greece

Abstract *The contributions of this article are the analysis and economic evaluation of the impact on tank wall losses of a diameter reduction of low-voltage bushings of pole-mounted single-phase distribution transformers. Finite element simulations of 5- to 167-kVA transformers were performed. The study was motivated when bushing manufacturers reduced diameter from 4.6 to 3.6 cm. Results show that when the diameter of low-voltage bushings is reduced, (i) load losses increase and (ii) total owning cost decreases for transformers up to 15 kVA and increases for transformers of 25–167 kVA. The insertion of non-magnetic material between bushing holes is also evaluated.*

Keywords pole-mounted distribution transformer, tank wall, load losses, efficiency, finite element method, total owning cost, low-voltage conductor, bushings

1. Introduction

Load losses in transformers have a component of losses due to the presence of eddy currents in the tank zone that surrounds the bushings [1–3]. This effect can be ignored on the high-voltage bushings, but on the low-voltage side, the currents are high and the closeness of low-voltage conductors to the tank wall has an important impact on load losses [4–8].

In 2005, Mexican bushing manufacturers reduced the diameter of low-voltage bushings used in distribution transformers to reduce manufacturing costs and, consequently, selling price to transformer manufacturers, but they did not evaluate the impact of this change in load losses.

Received 24 September 2010; accepted 3 April 2011.
Address correspondence to Prof. Juan C. Olivares-Galvan, Departamento de Energia, Universidad Autonoma Metropolitana-Azcapotzalco, Av. San Pablo no. 180, Col. Reynosa Tamaulipas, Delegacion Azcapotzalco, Mexico City, 02200, Mexico. E-mail: jolivare_1999@yahoo.com

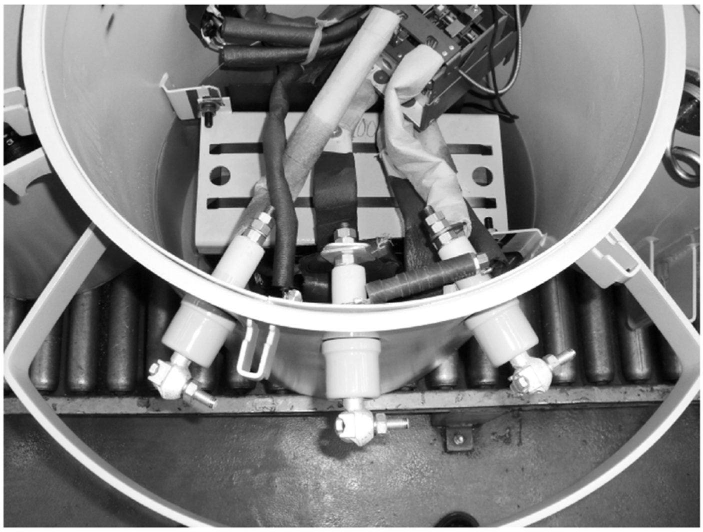

Figure 1. Three bushings for low-voltage conductors in the tank of a pole-mounted single-phase distribution transformer.

The main contribution of this work is the evaluation of the impact on tank wall losses of a reduction from 4.6 cm to 3.6 cm in the diameter of low-voltage bushings of 5 to 167-kVA, 33,000–240/120-V, pole-mounted, single-phase transformers. A review of tank wall losses on the low-voltage side of other types of distribution transformers was presented in [2].

Figure 1 shows a top view of an uncovered pole-mounted single-phase distribution transformer, where the low-voltage bushings can be observed as well as part of the core-windings and oil. The interior view of the same transformer is shown in Figure 2, where the holes for the low-voltage bushings can be observed.

Losses generated in the tank steel surrounding the transformer bushings can be the cause of hot spots that can damage the transformer oil and gaskets, jeopardize the maintenance staff and peripheral equipment, and could put the transformer out of service.

Figure 2. Interior view of tank of a pole-mounted single-phase distribution transformer.

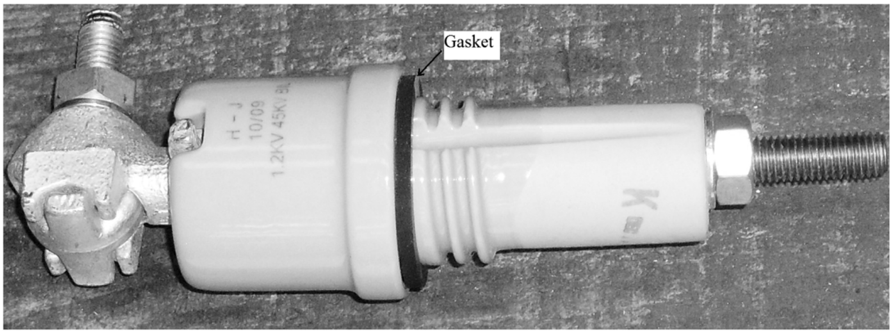

Figure 3. Low-voltage bushing with 3.6-cm diameter for pole-mounted distribution transformers.

Hot spots in transformers are one of the most important parameters that determine their lifetime. Transformers are designed and built to prevent overheating and premature failure [9–12].

Figure 3 shows a low-voltage bushing used for distribution transformers. Eddy currents induced in the transformer tank wall close to low-voltage bushings depend on several parameters, but the most important are the current magnitude, the diameter of bushing holes, and the tank wall properties (permeability and conductivity). Figure 4 shows the diagram of the 120-V connection used in all simulations and calculations, as it represents the most critical case.

In this study, the losses generated by full load currents flowing through the low-voltage conductors on transformer tank wall are calculated using three analytical formulas and the finite element method (FEM). The following section describes the analytical

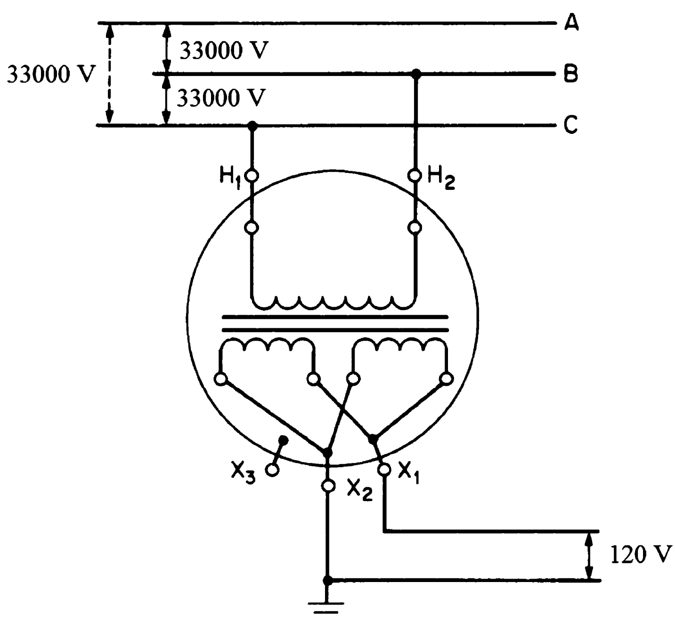

Figure 4. 120-V connection for pole-mounted distribution transformers.

formulas used to obtain tank losses, and in Section 3, the losses in the vicinity of the bushing holes are calculated with FEM simulations for 5- to 167-kVA transformers and for both 4.6- and 3.6-cm hole diameters.

2. Review of Existing Formulas to Calculate Losses Caused by a Current Crossing Through a Metallic Wall

This section presents three formulas to determine losses in metal plates due to their being crossed by currents. Each formula has particular characteristics. For example, there are two formulas that include the thickness of the metal plate and one that does not. Two formulas have a mathematical deduction, and one is empirical. These formulas are known as Turowski [4], Karsai [5], and Del Vecchio [6].

2.1. Turowski's Formula

The Turowski formula was derived in [4] using the geometry of Figure 5 to determine losses on a metal surface, in this case, a tank wall, that is crossed by a conductor carrying a current. Figure 5 shows the magnetic field components on a metallic plate that is crossed by conductors carrying a current. In Figure 5, D is the diameter of the bushing hole; A is the distance between bushing holes; l_1 is the longitude of the conductor from the tank cover to the conductor element dl; r is the distance from dl to P; dE_r, dE_θ, and dH are the electric and magnetic field components, respectively, of the dl element contributions at point P. The power P dissipated in a flat plate in terms of the magnetic field components is given by:

$$P = \zeta \frac{a_p}{2} \sqrt{\frac{\omega \mu_0}{2\gamma}} \iint_S \sqrt{\mu_{rs}(x, y)} |\boldsymbol{H}_{\boldsymbol{ms}}(x, y)|^{2x} dx dy, \tag{1}$$

where

S is the metallic plate surface;
ζ is a screening coefficient of field incidence on active power on the wall;
$\omega = 2\pi f$;
γ is the conductivity;

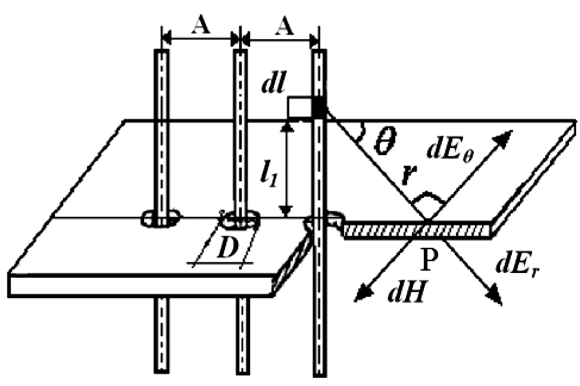

Figure 5. Magnetic field components of a metal surface (transformer tank) (copyright *1997 Proceedings of IEE Electric Power Applications* [4], reprinted with permission).

$a_p \approx 1.4$ is a linearization coefficient of relative permeability μ_{rs} that changes inside the solid steel for fields with $\boldsymbol{H_{ms}}$ larger than 5 A/cm;
x is unity for non-magnetic metals; and
$x \approx 1.05$ to 1.14 for steel.

Turowski's formula is obtained by simplifying the analytical expression of Eq. (1) [4]:

$$P \approx 3.15 \times 10^{-2} I^2 \sqrt{\frac{\omega\mu}{\sigma}} \left(0.74 + \ln \frac{2A}{D}\right). \tag{2}$$

Equation (2) is in terms of conductivity and permeability of the metallic plate that represents the tank wall. Other important parameters are the current flowing through the conductors, the diameter of the holes where the conductors go through, and the distance between the holes in the metallic tank wall. Turowski's formula, based on Poynting's theorem, does not explicitly include the metallic plate thickness.

2.2. *Karsai's Formula*

Karsai's formula [5] determines the power loss for a simplified model. This formula considers the hole diameter of bushings (D) and current density in the conductor (I), and it is only valid for magnetic steel of conductivity $\sigma = 7 \times 10^6$ S/m and magnetic flux density saturation $\boldsymbol{B_{SAT}} = 1.4$ T. These fixed values eliminate the possibility of using this formula to evaluate other materials. Also a drawback is the absence of the metallic wall thickness. Karsai's formula is given as [5]:

$$P = 405 \left(0.7 - \sqrt{\frac{D}{2}}\right) I^{1.5}. \tag{3}$$

2.3. *Del Vecchio's Formula*

The analytical formula of Del Vecchio includes the metallic tank wall thickness and is based on a circular plate of radio r crossed by an electrical conductor in the center [6].

In [6], Del Vecchio's formula is derived from Maxwell's equations in cylindrical coordinates:

$$\frac{1}{r}\frac{\partial}{\partial_r}\left(r\frac{\partial \boldsymbol{H_\phi}}{\partial_r}\right) - r\frac{\boldsymbol{H_\phi}}{r^2} + \frac{\partial^2 \boldsymbol{H_\phi}}{\partial z^2} = j\omega\mu\sigma \boldsymbol{H_\varphi}. \tag{4}$$

The tank losses of the transformer are given by [6]:

$$Loss_{bush} = 2\pi \int_a^b \int_{-c/2}^{c/2} \frac{|J_r|^2}{\sigma} r dr dz, \tag{5}$$

where a is the bushing hole radius, b is the external radius of the model plate, c is the wall thickness, and σ is the conductivity. The current density J induced in the tank can be found from Eq. (4). The integration of Eq. (5) yields Del Vecchio's formula used to determine the eddy current losses:

$$Loss_{bush} = \frac{I^2 q}{\pi\sigma} \ln\left(\frac{b}{a}\right) \left[\frac{\sinh(qc) - \sin(qc)}{\cosh(qc) + \cos(qc)}\right], \tag{6}$$

where $q = \sqrt{\frac{\omega\mu\sigma}{2}}$. A more simplified form of Eq. (6) when the product qc is small is given by [6]:

$$Loss_{bush} = \left(\frac{\pi}{6}\right)\frac{I^2 f^2 \mu^2 c^3}{\rho}\ln\left(\frac{b}{a}\right). \quad (7)$$

2.4. Review of Formulas

The results obtained using Del Vecchio's equation (Eq. (6)) for 4.6-cm and 3.6-cm bushing diameters show a difference of 4.51 W, 8.02 W, and 22.38 W in tank losses for each bushing for single-phase distribution transformers of 75 kVA, 100 kVA, and 167 kVA, respectively. The loss is calculated with the following parameters: $b = 0.91$ m, $c = 0.003$ m, $\mu = 500 \times 4\pi \times 10^{-7}$ H/m, and $\sigma = 5 \times 10^6$ S/m for a 120-V connection at $f = 60$ Hz. Table 1 presents the computed eddy current loss using Del Vecchio's Eq. (6) for bushing diameter $D = 46$ mm and $D = 36$ mm for the whole range of nine transformer ratings.

3. Calculation of Tank Wall Losses Using FEM

Several FEM simulations using Maxwell Ansoft 3D (ANSYS, Canonsburg, Pennsylvania, USA) were performed to determine the load losses change when the diameter of the low-voltage bushings is reduced from 4.6 to 3.6 cm. Results consider nine pole-mounted, single-phase distribution transformers rated 5 to 167 kVA for the 120-V connection (Figure 4).

The boundary conditions at the exterior surfaces of the finite-element model are specified with a zero tangential magnetic field condition. The direct modeling of eddy current regions usually leads to very expensive finite-element meshes, since the skin depth ($\delta = \sqrt{2/(\omega\mu\sigma)}$) of massive conductors at power frequencies is very small compared with the main dimensions of the electromagnetic device [13]. An alternative and very convenient way of modeling eddy current regions can be established with the use of

Table 1
Eddy current losses (W) using Del Vecchio's equation (Eq. (6)) for 5- to 167-kVA transformers; only one low-voltage bushing is considered

Transformer rating (kVA)	Losses (W) for $D = 46$ mm	Losses (W) for $D = 36$ mm
167	335.76	358.14
100	120.39	128.41
75	67.72	72.23
50	30.09	32.10
37.5	16.93	18.05
25	7.52	8.02
15	2.70	2.88
10	1.20	1.28
5	0.3	0.32

surface impedance boundary conditions [14–18], where a relationship between the tangential components of the magnetic field intensity **H** and the electric field **E** is established using the analytic solution of the field distribution in a semi-infinite conducting slab. The practical implementation of this approach is to relate the tangential component of the magnetic field intensity $\mathbf{H}_{st}$ with the electric field $\mathbf{E}_{st}$ at the eddy-current region surface using [2]:

$$\mathbf{E}_{st} = Z_s(\mathbf{n} \times \mathbf{H}_{st}), \quad (8)$$

where $Z_s = \frac{1+j}{\sigma\delta}$ and **n** is a normal unity vector (outward) to the conductor surface. Equation (8) amounts to the specification of a boundary condition, which eliminates the necessity of actual modeling of the eddy current regions and only requires that the surface of the material be covered with finite elements.

3.1. Validation of the Model

Results in [6] were used to validate simulations. Calculation of eddy current losses is performed on a carbon steel disk, shown in Figure 6(a), with an inner diameter of 0.132 m, an outer diameter of 0.305 m, a thickness of 0.0095 m, a relative permeability of $\mu_r = 200$, an electrical conductivity of $\sigma = 4 \times 10^6$ S/m, and a conductor made of copper with $\mu_r = 1$ and $\sigma = 58 \times 10^6$ S/m. The distribution of loss density in W/m^2 of the model is shown in Figure 6(b).

Total losses (W) of the disk were obtained by [6]:

$$Loss = \sqrt{\frac{\omega\mu_r\mu_o}{8\sigma}} \int_{surface} \boldsymbol{H}_t \bullet \boldsymbol{H}_t^* ds, \quad (9)$$

where $\boldsymbol{H}_t$ is the tangential magnetic field strength (A/m), $\boldsymbol{H}_t^*$ is its conjugate, μ_r is the relative permeability, μ_o is the vaccum permeability ($4\pi \times 10^{-7}$ H/m), σ is the electric conductivity (S/m), and ω the angular frequency (rad/s).

Integration of Eq. (9) on both sides of the disk results in 1117.92 W of total losses in the disk. This represents an error of 2% compared with the result reported in [6].

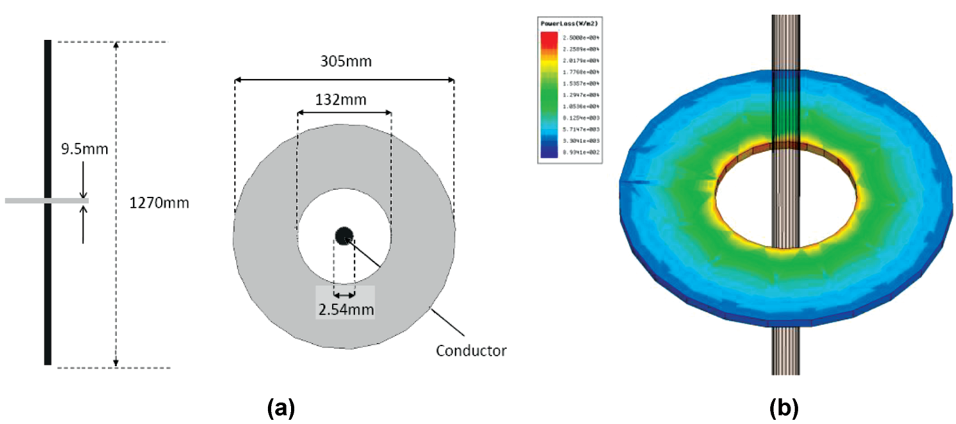

Figure 6. (a) Steel disk geometry to determine eddy current losses generated by current crossing it [6] and (b) distribution of loss density in W/m^2 on the metal disk. (color figure available online)

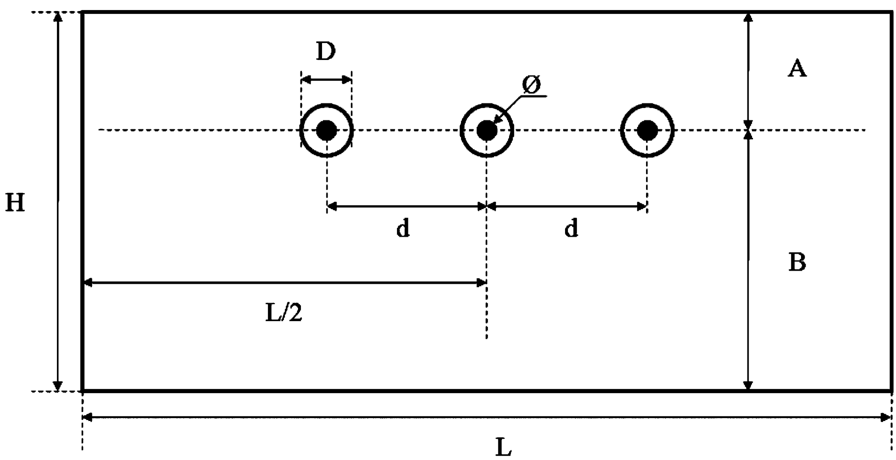

Figure 7. Carbon steel flat plate.

3.2. Curved and Flat Steel Plate with 4.6-cm-diameter Holes

In this section, the FEM is used to obtain losses in a carbon steel curved plate of 2.28 mm (13-gauge) thickness with holes 4.6 cm in diameter, $\mu_r = 500$, and $\sigma = 5 \times 10^6$ S/m [7], which corresponds to the zone where the low-voltage bushings are placed on the tank of pole-mounted distribution transformers. The curved metal plate is modeled with a half cylinder using a dodecagon, as flat surfaces are needed to use an impedance boundary. The results are compared with those obtained for a flat plate. The difference of the losses obtained for the flat plate in comparison with the losses of the curved plate, when the simulations are performed for the actual dimensions of the transformer as well as the same bushing holes diameter, is considered as a percentage error.

Figure 7 shows the geometry of the flat plate with three holes and their respective conductors. The dimensions of the flat plate and conductor diameter for the different ratings are given in Table 2. Each conductor is modeled by a polygon of 24 sides, and the current considered is the peak value of the rated current of a single-phase distribution transformer for a 120-V connection.

Table 2
Dimension of the steel plate shown in Figure 7

	Transformer rating (kVA)								
	5	10	15	25	37.5	50	75	100	167
H (cm)	61	61	68	71	71	73	73	73	73
L (cm)	99	105	110	123	135	152	165	178	187
A (cm)	16	21	21	21	21	21	21	21	21
B (cm)	45	40	47	51	51	52	52	52	52
D (cm)	4.6/3.6	4.6/3.6	4.6/3.6	4.6/3.6	4.6/3.6	4.6/3.6	4.6/3.6	4.6/3.6	4.6/3.6
Ø (mm)	9.906	9.906	9.906	9.906	11.938	11.938	11.938	11.938	11.938
d (cm)	12	12	12	13	13	13	13	13	13

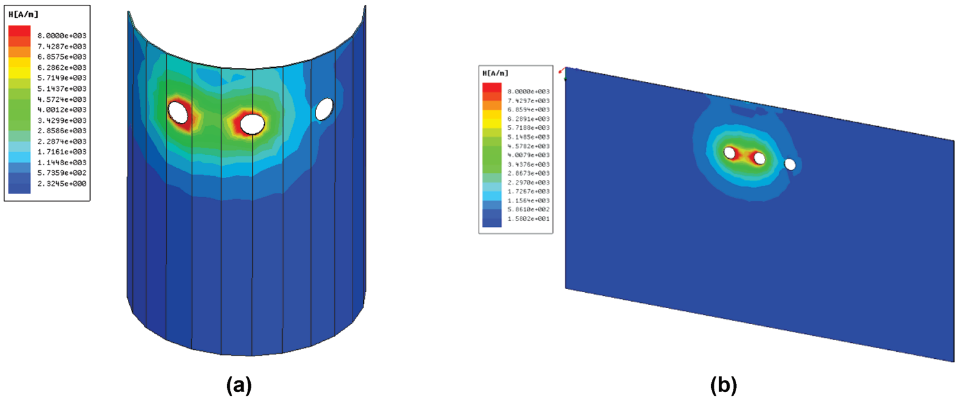

Figure 8. Distribution of magnetic field intensity for a 100-kVA transformer with 4.6-cm-diameter bushing holes: (a) curved metal plate and (b) flat metal plate. (color figure available online)

Figure 8 shows peak values of magnetic field intensity distribution on both a curved and a flat metal plate for a 100-kVA transformer with 4.6-cm-diameter bushing holes.

It can be observed from Figure 8(a) that the distribution of magnetic field intensity for the curved plate has the same pattern as the one obtained when simulation was performed with a flat plate with holes of same diameter (Figure 8(b)), both with a high magnetic field intensity located around the holes. Figure 9(a) shows the loss density distribution in W/m^2 on the curved plate for the 100-kVA transformer with 4.6-cm-diameter bushing holes, which is very similar to the distribution shown in Figure 9(b) for the flat plate.

For the case of the curved plate with 4.6-cm holes, total losses calculated with Eq. (9) for the 100-kVA transformer were 118.78 W. The value obtained with the flat-plate model with the same diameter holes was 116.61 W, which means a difference of 2.17 W (1.8%). To validate the use of the flat-plate geometry in all ratings, two simulations for the 50- and 167-kVA ratings were performed and found that the highest percentage error is 6.04%.

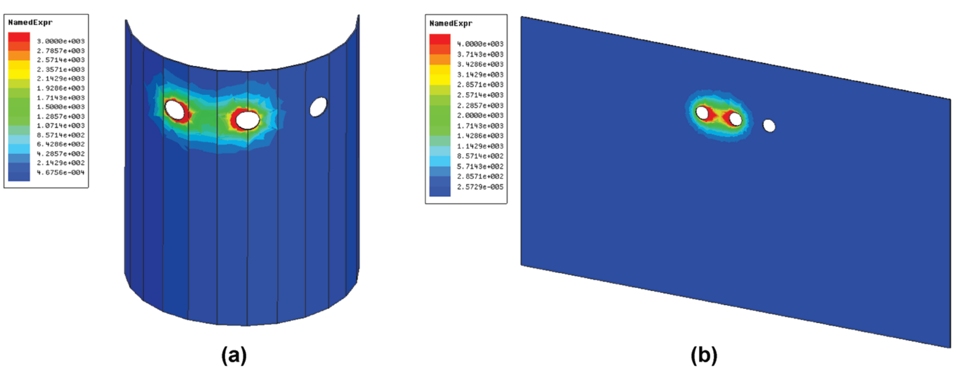

Figure 9. Distribution of loss density in W/m^2 on the for 4.6-cm-diameter bushing hole of a 100-kVA transformer: (a) curved plate and (b) flat plate. (color figure available online)

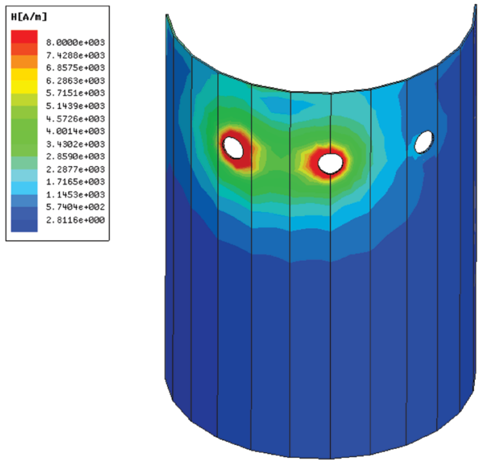

Figure 10. Distribution of magnetic field intensity on the curved plate for 3.6-cm-diameter bushing hole 100-kVA transformer. (color figure available online)

3.3. Curved and Flat Steel Plate with 3.6-cm-diameter Holes

The mesh of the curved steel plate with three 3.6-cm-diameter bushing holes is of the same design as for the 4.6-cm diameter. Figure 10 shows the peak values of distribution of magnetic field intensity in the curved plate for a 100-kVA transformer with 3.6-cm-diameter bushing holes.

Figure 11 shows the loss density distribution in W/m^2 on the curved plate for a 100-kVA transformer with 3.6-cm-diameter bushing hole. Total losses for the curved plate with 3.6-cm-diameter bushing holes for the 100-kVA transformer were 135.77 W using Eq. (9). The value obtained with the flat-plate model with the same diameter bushing holes and same dimensions of transformer was 133.82 W. The difference of the losses

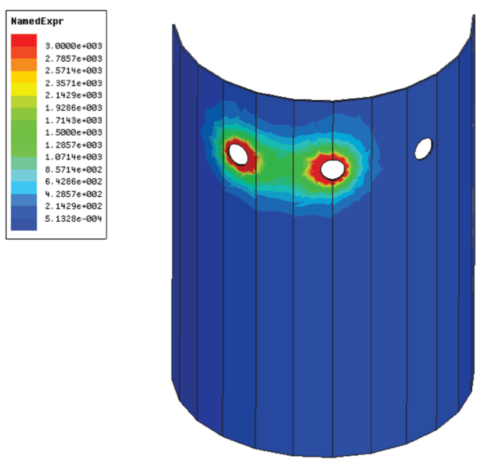

Figure 11. Distribution of loss density in W/m^2 on the curved plate for 3.6-cm-diameter bushing hole 100-kVA transformer. (color figure available online)

Table 3
Tank wall loss increase and TOC increase for nine transformer ratings when the bushing diameter is decreased from 4.6 cm to 3.6 cm

	Tank wall loss increase		TOC increase	
kVA	W	(%)	$	%
167	56.65	5.52	223.12	2.40
100	17.21	2.91	64.57	1.05
75	10.88	1.97	39.12	0.75
50	4.84	1.28	14.84	0.39
37.5	1.58	0.55	1.74	0.06
25	1.71	0.79	2.26	0.10
15	0.40	0.27	−3.01	−0.18
10	0.23	0.23	−3.69	−0.30
5	0.07	0.10	−4.33	−0.54

obtained with the flat plate and the curved plate for this rating represents an error of 1.43%. Errors for 50- and 167-kVA transformers were also small (less than 6%). Hence, a contribution, from the engineering point of view, is the possibility to calculate tank losses with the flat-plate geometry for all ratings.

3.4. *Comparison of Losses and Total Owning Cost (TOC)*

The results of loss differences obtained from FEM simulations for 5- to 167-kVA transformers with 120-V low-voltage connection when considering the change of bushings diameter from 4.6 to 3.6 cm are shown in Table 3, the percentage of increase is expressed with respect to load losses for 4.6-cm bushings' diameter. The maximum obtained difference of tank losses in the nine transformer ratings is 56.65 W for the 167-kVA transformer for a low-voltage current of 1968.14 A. Table 4 shows the TOC results for the same nine transformer ratings for 3.6- and 4.6-cm bushing holes

Table 4
Technical characteristics of nine transformer ratings with 36/46-mm bushing diameter

		Load loss (W)		Material cost ($)		Bid price ($)		TOC ($)	
kVA	No-load loss (W)	46 mm	36 mm	46 mm	36 mm	46 mm	36 mm	46 mm	36 mm
167	311.79	1025.4	1082.05	1708.53	1705.53	2628.51	2623.89	9294.82	9517.94
100	217.6	592.05	609.26	1306.97	1303.97	2010.72	2006.11	6166.38	6230.95
75	184.96	551.24	562.12	957.89	954.89	1473.68	1469.06	5198.94	5238.06
50	134.8	377.98	382.82	757.74	754.74	1165.75	1161.14	3785.20	3800.04
37.5	113.59	285.52	287.1	684.33	681.33	1052.82	1048.20	3127.50	3129.24
25	84.57	216.55	218.26	511.58	508.58	787.05	782.43	2347.67	2349.93
15	59.69	150.9	151.3	355.86	352.86	547.48	542.86	1641.17	1638.16
10	46.84	99.21	99.44	294.65	291.65	453.31	448.69	1234.35	1230.66
5	28.98	68.01	68.08	185.44	182.44	285.29	280.68	795.17	790.84

diameter and for aluminum-aluminum transformers (aluminum cost = \$1.869/kg, London Metal Exchange (LME) officials, 2 November 2009; source: MetalPrices.com). All parameters were computed by transformer design optimization software [1]. The TOC is calculated with

$$TOC = BP + CL = BP + A \cdot NLL + B \cdot LL, \tag{10}$$

where

A = US\$8.16/W (no-load loss cost rate) and B = US\$4.02/W (load loss cost rate), which are current values for Mexican utilities [19];
BP (\$) is the bid price of the transformer;
CL (\$) is the cost of transformer losses throughout the transformer lifetime considering 25 years;
NLL (W) is transformer no-load loss; and
LL (W) is transformer load loss.

Readers can find A and B for 26 countries in [20].

The negative sign in the TOC increase of 5-, 10-, and 15-kVA transformers in Table 3 means that the reduction in bushing price is bigger than the increment of operation cost due to the load losses increase. On the other hand, TOC increase in transformers bigger than 15 kVA and up to 167 kVA means that the reduction of bushing holes diameter represents a cost disadvantage due to the rise of operation cost.

3.5. Non-magnetic Insert Between Bushings

Finally, a simulation for an arrangement that includes a strip of non-magnetic material between bushing holes was performed. Figure 12(a) shows the distribution of magnetic field intensity in the curved plate for a 100-kVA transformer with a 3.6-cm-diameter bushing hole when a strip of non-magnetic material 4.76 mm wide is inserted between holes. The thickness of the non-magnetic strip is the same as that of the transformer

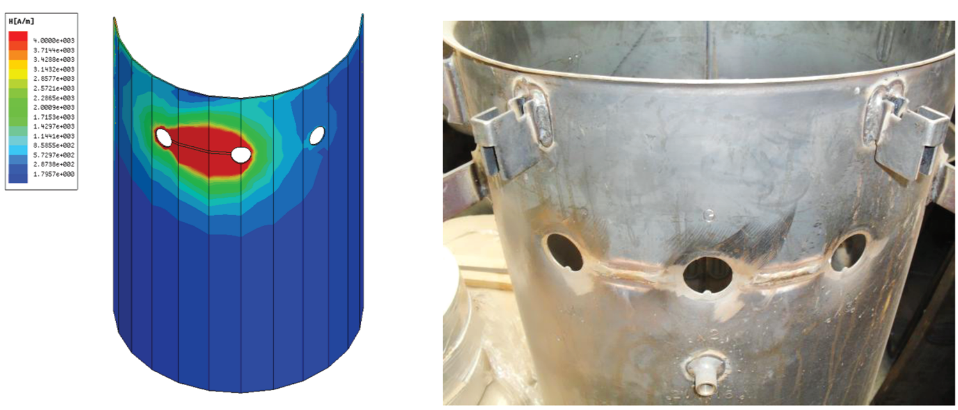

(a) (b)

Figure 12. (a) Distribution of magnetic field intensity on the curved plate for 3.6-cm bushing hole diameter of 100-kVA transformer including non-magnetic insert and (b) physical aspect of non-magnetic insert on a transformer tank. (color figure available online)

Table 5
Tank wall losses decrease for nine transformer ratings when diameter of bushings is 3.6 cm and non-magnetic inserts are used

	Tank wall loss decrease	
kVA	W	%
167	155.34	14.36
100	66.17	10.86
75	37.26	6.63
50	7.45	1.95
37.5	4.86	1.69
25	2.67	1.22
15	0.63	0.42
10	0.22	0.22
5	0.05	0.07

tank (see Figure 12(b)). Table 5 contains tank wall losses reduction for all analyzed ratings with the non-magnetic insert. It can be seen that for the 167-kVA transformer, losses decrease 155 W (Table 5). The percentage of decrease is expressed with respect to load losses. Non-magnetic inserts were manufactured using 41.536 grams of E309L UTP 309L stainless-steel electrodes (Todo para soldar en linea, Nuevo Leon, Mexico) with a cost of \$0.58 per transformer (labor and energy costs are not included). The labor time for welding process was 3 min and 30 sec per transformer.

4. Conclusions

The need to analyze the impact of changes in the bushing diameter on transformer load loss is the motivation for this article. The performed analysis compares tank losses in geometries of models of the tank zone that surrounds the low-voltage bushings of pole-mounted distribution transformers. The selected technique to evaluate the losses was the FEM. The models to perform the simulations were mainly designed to give information on the difference of tank losses with bushings that have a diameter of 4.6 cm and those with a diameter 3.6 cm. The surface impedance boundary condition was used in the simulations, as it only requires that the surface of the material be covered with finite elements, providing a very convenient means of including the effect of a non-linear B-H material characteristic. Tank losses obtained with FEM simulations for the analyzed cases show that a flat-plate model can be used to determine tank losses, as the difference in losses calculated with flat or curved metallic plate is less than 6%.

The comparative study shows that for 5-, 10-, and 15-kVA transformers, there is a marginal cost advantage when the diameter of bushing is reduced. For 25- and 37.5-kVA transformers, there is no appreciable cost difference with the diameter reduction. This finding represents the possibility of a reduction of manufacturing cost of pole-mounted distribution transformers of 37.5 kVA or smaller without an increase in the operation (losses) cost when using bushings of 3.6-cm diameter. This is not the case for 50- to 167-kVA transformers, where there is an important difference in tank losses when the diameter of low-voltage bushings is reduced from 4.6 cm to 3.6 cm, *e.g.*, the increase of transformer tank losses for the 167-kVA rating is 56.65 W. This difference increases with transformer rating and life expectancy.

For single-phase distribution transformers, manufactured in large numbers, the use of non-magnetic stainless steel can result in considerable energy savings. A stainless-steel insert between holes was found to be effective in appreciably reducing the load loss on nine ratings (5 kVA to 167 kVA) of single-phase transformers. The extra cost of the non-magnetic stainless steel can be recovered in about a year, due to the energy savings for a 50-kVA transformer. The non-magnetic stainless steel is recommended for transformer ratings above 37.5 kVA.

References

1. Georgilakis, P. S., *Spotlight on Modern Transformer Design*, 1st ed., London, UK: Springer, Chap. 2, pp. 94–99, 2009.
2. Olivares-Galván, J. C., Georgilakis, P. S., and Ocon-Valdez, R., "A review of transformer losses," *Elect. Power Compon. Syst.*, Vol. 37, No. 9, pp. 1046–1062, September 2009.
3. López-Fernández, X. M., Penabad-Duran, P., and Turowski, J., "3-D methodology for the heating hazard assessment on transformer cover," *XIX International Conference on Electrical Machines (ICEM)*, Rome, 6–8 September 2010.
4. Turowski, J., and Pelikant, A., "Eddy currents losses and hot-spot evaluation in cover plates of power transformers," *Proc. Inst. Elect. Eng. Elect. Power Appl.*, Vol. 144, No. 6, pp. 435–440, November 1997.
5. Karsai, K., Kerényi, D., and Kiss, L., *Large Power Transformers*, New York: Elsevier Science Publisher, Chap. 4, p. 178, 1987.
6. Del Vecchio, R. M., Poulin, B., Feghali, P. T., Shah, D. M., and Ahuja, R., *Transformer Design Principles*, New York: Taylor & Francis, NY, pp. 412–418, 2002.
7. Ahuja, R., and Del Vecchio, R. M., "Transformer stray loss and flux distribution studies using 3D finite element analysis," *Proc. Inst. Elect. Eng. Elect. Power Appl.*, Vol. 144, pp. 435–440, 1997.
8. Kim, D. H., and Hahn, S. Y., "Improved design of cover plates of power transformers for lower eddy current losses," *IEEE Trans. Magnet.*, Vol. 35, No. 5, pp. 2529–3531, September 1999.
9. Nims, J. W., Smith, R. E., and El-Keib, A. A., "Application of a genetic algorithm to power transformer design," *Elect. Power Compon. Syst.*, Vol. 24, No. 6, pp. 669–680, 1996.
10. Singh, B., and Saxena, R. B., "Optimum design of small distribution transformer using aluminium conductors," *Elect. Power Compon. Syst.*, Vol. 12, No. 4, pp. 271–280, 1987.
11. Kowalski, J., and Pylak, K., "Polyoptimization problem in power core type transformer design," *Elect. Power Compon. Syst.*, Vol. 21, No. 4, pp. 493–506, 1993.
12. Hernández, I., de León, F., Cañedo, J. M., and Olivares-Galván, J. C., "Modelling transformer core joints using Gaussian models for the magnetic flux density and permeability," *IET Elect. Power Appl.*, Vol. 4, No. 9, pp. 761–771, 2010.
13. Kumbhar, G. B., Mahajan, S. M., and Collett, W. L., "Reduction of loss and local overheating in the tank of a current transformer," *IEEE Trans. Power Delivery*, Vol. 25, No. 4, pp. 2519–2525, October 2010.
14. Sakellaris, J., Meunier, G., Gurin, C., and Sabonnadiere, J. C., "Application of the impedance boundary condition in a finite element environment using the reduced potential formulation," *IEEE Trans. Magnet.*, Vol. 27, No. 6, pp. 5022–5024, November 1991.
15. Rodger, D., and Lai, H. C., "A surface impedance method for 3-D time transient problems," *IEEE Trans. Magnet.*, Vol. 35, No. 3, pp. 1369–1371, May 1999.

16. Sabariego, R. V., Dular, P., Geuzaine, C., and Gyselinck, J., "Surface-impedance boundary conditions in dual time-domain finite-element formulations," *IEEE Trans. Magnet.*, Vol. 46, No. 8, pp. 3524–3531, August 2010.
17. Holland, S. A., O'Connell, G. P., and Haydock, L., "Calculating stray loss in power transformers using surface impedance with finite elements," *IEEE Trans. Magnet.*, Vol. 28, No. 2, pp. 1355–1358, March 1992.
18. Jingguo, W., Lavers, J. D., and Peibai, Z., "Modified surface impedance boundary condition applied to eddy current problems," *IEEE Trans. Magnet.*, Vol. 28, No. 2, pp. 1197–1200, March 1992.
19. Olivares-Galván, J. C., de León, F., Georgilakis, P. S., and Escarela-Perez, R., "Selection of copper versus aluminum windings for distribution transformers," *IET Elect. Power Appl.*, Vol. 4, No. 6, pp. 474–485, 2010.
20. Baehr, R., "Transformer technology state-of-the-art and trends of future development," Electra No. 198, October 2001.